Chapter 8 RADAR -

A Imaging radar

Radar, specifically imaging radar, provides a powerful tool for remote sensing. The two primary advantages are the 24 hour capability (independence from solar illumination), and all-weather (cloud penetration) capability. Radar can penetrate to modest depths into the earth, and can occasionally allow glimpses below the surface of the earth. This is useful for detecting buried objects, such as pipelines or mines. Polarization becomes a very powerful tool in the SAR domain.

Radar images were shown in Chapter 1, and an airborne image is shown here in Figure 8.1. The image of San Francisco is done in two wavelengths, encoded in complementary blue/yellow tones. Most of the urban surfaces reflect equally well in the two wavelengths, and much of the scene is shades of gray (white).

Figure 8-1. San Francisco, California, JPL AIRSAR, C and L band, VV polarization. October 18, 1996, 71351 seconds GMT. Ten meter GSD, aircraft tack -135°.

B Theory

1 Imaging Radar Basics

Before discussing the operation of an imaging radar system, it is appropriate to discuss the terminology and characteristics for imaging radar. Illustrations are used for Side-Looking Airborne Radar (SLAR). As shown in Figure 8-2, an airplane or spacecraft moves at some velocity and at some altitude in an azimuth, or along-track direction. Through a fixed antenna, pulses of microwave radiation are propagated outward in a perpendicular plane at the speed of light in the range, look or across-track direction. Slant range is the line-of-sight distance measured from the antenna to the terrain target, whereas ground range is the horizontal distance measured. along the surface from the ground track, or nadir line, to the target. The area closest to the ground track at which a radar pulse intercepts the terrain is the near range, and the area of pulse termination farthest from ground track is the far range.

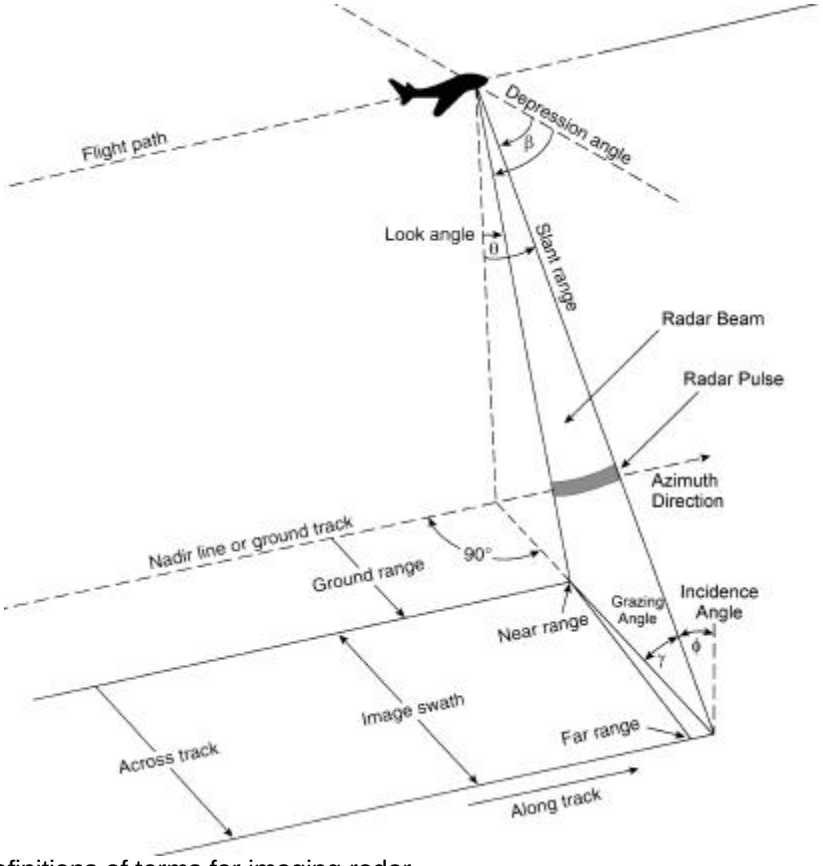

Figure 8-2. Definitions of terms for imaging radar.

The angle measured from a horizontal plane downward to a specific part of the radar beam defines the depression angle (β). The depression angle varies across the image swath from relatively steep (large angle) at near range to relatively shallow (small angle) at far range. The angle measured from a vertical plane upward to a specific part of the radar beam defines the look angle (θ). The look angle varies across the image swath from a relatively small angle at near range to a relatively large angle at far range. When

measured to the same part of the beam, the depression angle and the look angle are complementary angles ($\beta + \theta = 90°$).

The **incidence angle (**f**)** is the angle measured between the axis of the radar beam and a line perpendicular to the local ground surface that the beam strikes; the complement of the incidence angle is called the **grazing angle (**g**).** Consequently, the incidence angle and the grazing angle are a function of both the illumination angle (β or θ) and the slope of the terrain. When the terrain is horizontal, the depression and grazing angles are equal ($\beta = \gamma$) and the look and incidence angles are equal ($\theta = \phi$).

A key parameter often used to judge the quality of a radar image is resolution. Radar resolution is defined as the minimum separation between two objects of equal reflectivity that will enable them to appear individually in a processed radar image. The most important criterion for establishing resolution is the size of the pulse rectangle projected onto the ground at a given instant of time. The pulse rectangle is similar to the ground resolution cell associated with across-track scanners. When two or more objects fall within the same pulse rectangle they cannot be resolved as separate entities. Rather, they are presented as one echo to the radar system. If objects are separated by a distance exceeding the corresponding dimension of the pulse rectangle, they will be imaged separately. The size of the pulse rectangle is controlled by two independent resolutions: (1) Range resolution determines resolution cell size perpendicular to the ground track and (2) azimuth resolution establishes the cell size parallel to the ground track. These relationships are discussed in the following sections.

2 Detection

Radar detection is a measure of the smallest object that can be discerned on an image as a result of its ability to reflect microwave radiation. Detection is often associated with highly reflective metal objects such as vehicles, railroad tracks, fences, and power lines and poles, which are physically much smaller than the pulse rectangle. For example, a vehicle is normally a much better reflector of microwave than its surroundings, making it the dominant reflector in the pulse rectangle. When this composite reflectance value differs from those in surrounding cells, the radar system, in essence, detects the vehicle. However, to the radar, the vehicle is as large as the cell size. Users are often amazed by the detail seen in radar images because many small features are detected when resolution is not required to distinguish them from surrounding objects (Matthews 1975).

3 Range Resolution

Range, or **across-track, resolution** in **slant range (R_{sr})** is determined by the physical length of the radar pulse that is emitted from the antenna; this is called the **pulse length (**t**).** If not given, pulse length can be determined by multiplying the pulse duration (δ), or the length of time in microseconds (1 μs= 1×10^{-6} s) that the pulse was emitted from the antenna by the speed of light ($c = 3\times10^{8}$ m/s **);**

$$\tau = \delta c. \qquad \text{(Eqn. 8.1)}$$

For a radar system to discern two targets in the across- track dimension all parts of their reflected signals must be received at the antenna at different times or they will appear as one large entity in an image. In Figure 8-3 it is seen that objects separated by a slant-range distance equal to or less than $\tau/2$ will produce reflections that arrive at the antenna as one continuous pulse, dictating that they be imaged as one large object (targets A, B, and C). If the slant-range separation is greater than $\tau/2$, the pulses from targets C and D will not overlap, and their signals will be recorded separately. Thus, slant-range resolution measured in the across- track dimension is equal to one-half the transmitted pulse length:

$$R_{sr} = \frac{c\,\tau}{2}. \qquad \text{(Eqn. 8.2)}$$

To convert R_{sr} to ground-range resolution (R_{gr}), the formula is:

$$R_{gr} = \frac{c\,\tau}{2\cos\beta} \qquad \text{(Eqn. 8.3)}$$

where: τ= pulse length, c is the speed of light, and β= antenna depression angle.

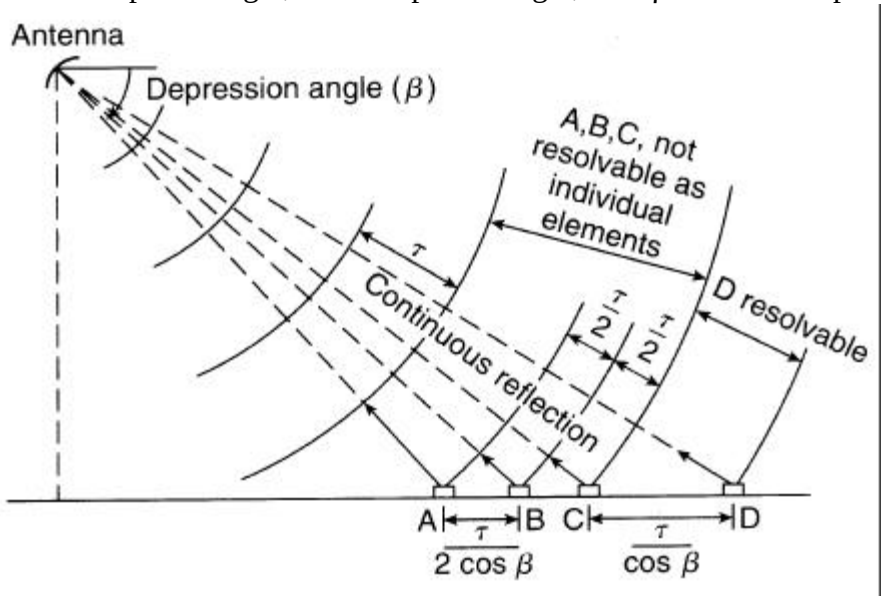

Figure 8-3. Range resolution is a function of pulse length

It can be noted from the equation that:

(1) ground- range resolution improves as the distance from the ground track increases (i.e., across-track resolution is better in far range than in near range because β is smaller), and

(2) resolution can be improved by shortening the pulse length. However, a point will be reached when a drastically shortened pulse will not contain sufficient energy for its echoes to be detected by the receiver.

A closely related concept to the pulse duration is the pulse repetition rate, or frequency (PRF). This corresponds to the interval between pulses, and is relatively long compared to the pulse duration. Figure 8-4 illustrates the signals used for the SIR-C x-band radar. Here, the pulse width is 40-μs, the PRF is 1240-1736 Hz, or about 15 times the width of the pulses illustrated here.

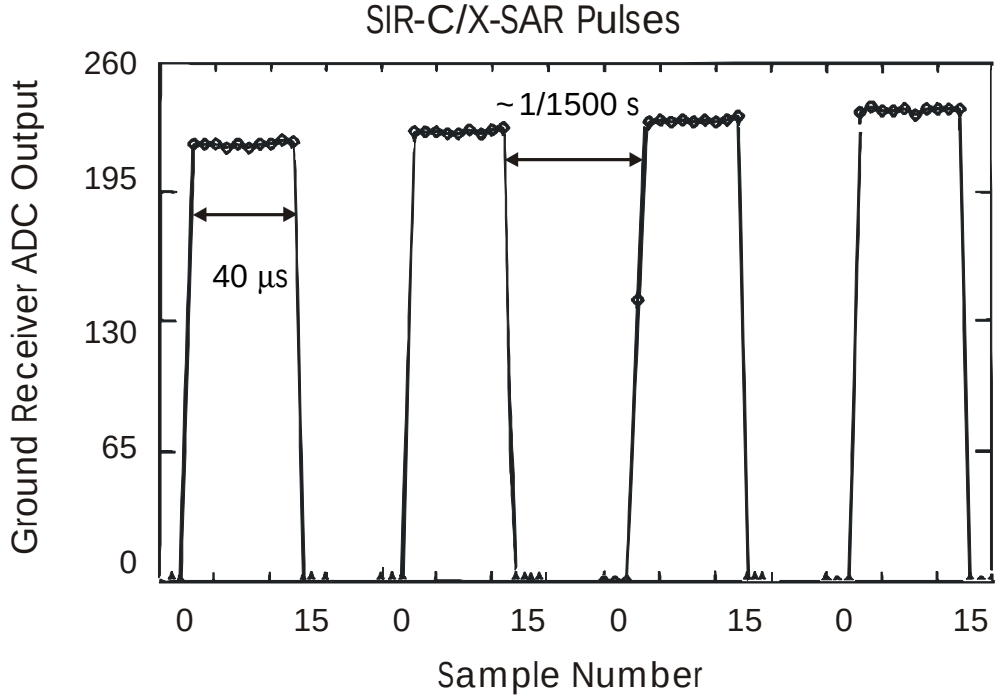

Zink & Bamler, X-SAR Radiometric Calibration and Data Quality, IEEE TGRS, July 1995

Figure 8-4. SIR-C X-SAR pulses recorded by a ground calibration receiver, sampling at 4 μs (250 kHz). Data Take 30 of SRL-1 (April, 1994). The slight variation in power seen over this interval is due to the progress of the shuttle over the ground site. Note that without signal shaping, the best range resolution which could be obtained from such pulses would be 6 km.

4 Signal Shape

Our ability to resolve targets basically revolves the length of the radar pulse - that is the spatial extent of the pulse. By manipulating the shape of the pulse, we can finesse the limitation which is imposed by our need to keep a fairly long pulse length, a requirement imposed by the power constraints of real radar. The limitation is resolved by modulating the frequency of the pulse, or using FM chirp, invented by Suntharalingam Gnanalingam at Cambridge to study the ionosphere. (Professor Gnanalingam worked at NPS from ~1985-1995). To understand the process, we need to look at radar pulses in both time and frequency space.

A closely related concept is the bandwidth associated with the pulse length. Figure 8-5 illustrates some basic features of signals, and the relationship between pulse length and the spread in frequencies associated with square pulses. Basically, if you have a very short pulse, a wide spectrum of frequencies is implicit, while a monochromatic signal implies a very long pulse. For an infinitely long pulse, one can have a monochromatic (single frequency) signal. For any square pulse, the transformed signal is a sinc function $\left(\frac{\sin x}{x}\right)$ centered at the carrier frequency. The bandwidth is basically (twice) the inverse of the pulse length.

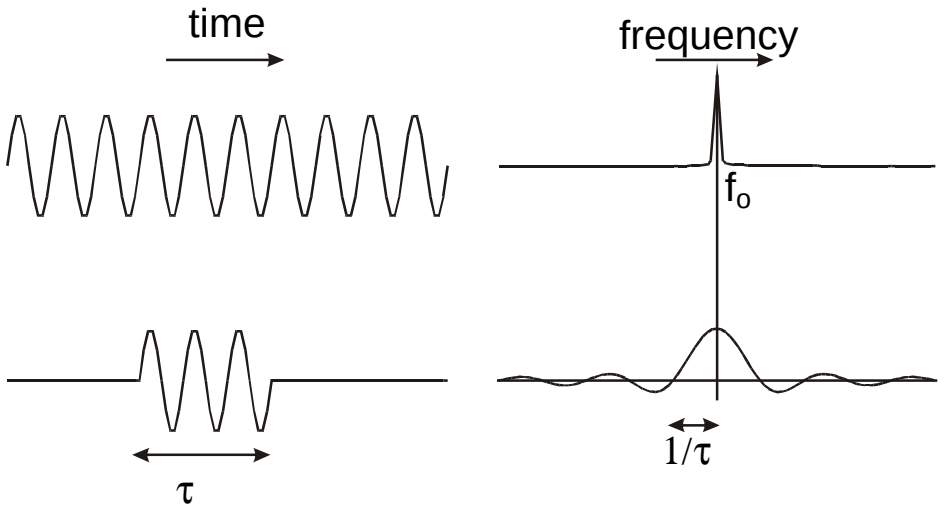

Figure 8.5 Continuous wave and pulsed signals. Note that bandwith = 2/pulse length. The plots on the right are Fourier transforms of the signals on the left.

Figure 8-6 illustrates the chirp concept - the frequency increases with time. Now, each cycle of the transmitted signal can by more or less uniquely identified by its frequency. Relatively long pulses can be used, and the width of the pulse in frequency space is now defined by the range of the chirp (Δf). This is illustrated in Figure 8.6. The Fourier transform of this signal is a nicely defined signal again centered at the carrier frequency, and with a width of Δf. Numbers for the SIR-C X-band were, for example f_0 = 9.6 GHz, and Δf = 20 MHz. What does this buy you? Though not shown here, the result you obtain from analysis is basically the same - the spatial resolution is defined by the pulse

length, which is the inverse of the bandwidth. With a chirped pulse, one replaces the bandwidth noted above (the inverse of the "real" pulse length), with the bandwidth of the chirp. One can obtain a spatial resolution which is defined by an effective time:

$$t = \frac{1}{\Delta f}. \qquad \text{(Eqn. 8.4)}$$

which in turn gives a range resolution as given in Equation 8.2.

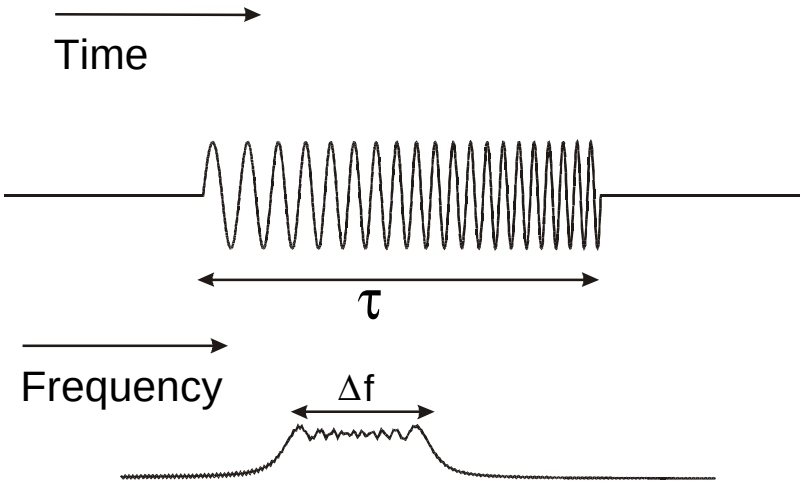

Figure 8.6 A pulse varies linearly in frequency from f to $f_o+\Delta f$, the power is then localized in frequency space (bandwidth). (Elachi, page 185)

As an illustration, the SIR-C X-band pulse length is 40 μs, which implies a bandwidth of

$BW = \frac{1}{4\times10^{-5}} = 2.5\times10^{4}$ Hz, and a range resolution of

$$R_{sr} = \frac{3\times10^{8} \bullet 4\times10^{-5}}{2} = 6\times10^{3} \text{ m}$$

using the 20 MHz chirp range for bandwidth, we get an effective pulse length of

$t = \frac{1}{\Delta f} = \frac{1}{2\times10^{7}} = 5\times10^{-8}$ s, and hence an effective slant range resolution of

$$R_{sr} = \frac{3\times10^{8} \bullet 5\times10^{-8}}{2} = 7.5 \text{ m}$$

The actual performance was not quite this good, as is generally found in real life.
The so-called "compression-ratio" is the ratio of the two times, which here is

$\frac{4\times10^{-5}}{5\times10^{-8}} = 8\times10^{2}$, or 800. Just as a reference, the European ERS-1 systems has a compression ratio of 575 on its 37.1-μs pulse, for an effective pulse duration of 64.5 ns.

---

5 Azimuth Resolution

Azimuth, or along-track resolution (R_a) is determined by the width of the terrain strip illuminated by a radar pulse, which is a function of the beamwidth of a real-aperture radar (RAR). In Figure 8-6 it is shown that the beamwidth increases with range. Thus, two tank-like objects (at the same range) are in the beam simultaneously, and their echoes will be received at the same time. Consequently, they will appear as one extended object in an image. Two other objects, an A7 jet and T72 tank, are located outside the beam width as shown here. Since a distance greater than the beamwidth separates them; their returns will be received and recorded separately. Thus, to separate two objects in the along-track direction, it is necessary that their separation on the ground be greater than the width of the radar beam. What determines the beam width? Basically the length of the antenna.

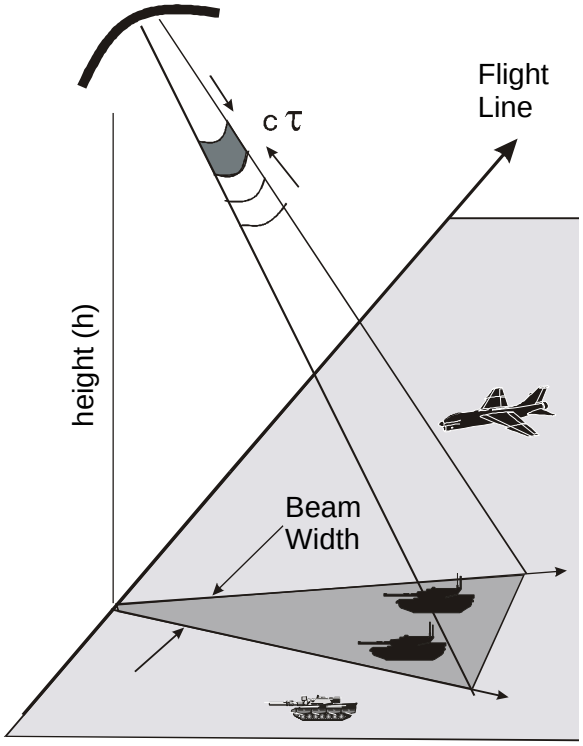

Figure 8-7

6 Beam Pattern and resolution

We need to look at the nature of the antenna radiation pattern briefly, in order to get a handle on the resolution characteristics of an imaging radar system. Following Elachi (pages 177-180), we consider the far field contribution of a radiator which is one member of a linear array.

$$E_n \approx \left[a_n e^{i\phi_n} \right] e^{-ikd_n \sin\theta} \qquad \text{(Eqn. 8.5)}$$

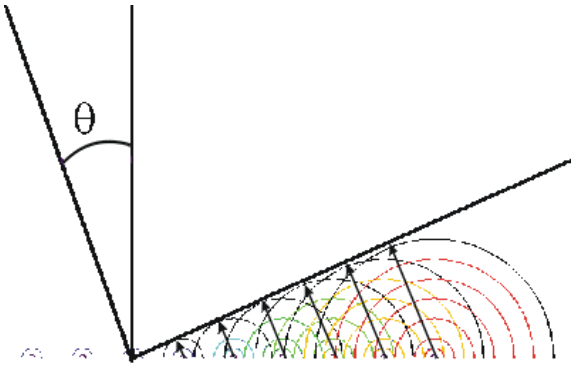

Figure 8-8. Elachi, page 177

The total field from all the radiators is the sum of the elements

$$E(\theta) \approx \sum_n a_n e^{i\phi_n - ikd_n \sin\theta} \qquad \text{(Eqn. 8.6)}$$

where each element contributes and amplitude a_n, and a phase ϕ_n. If the radiators are all identical in phase and amplitude, and equally spaced, then the total field is

$$E(\theta) \approx ae^{i\phi} \sum_{n=1}^{N} e^{-inkd \sin\theta} \qquad \text{(Eqn. 8.7)}$$

This sum is strongly dependent on the factor in the exponential, $\Psi = kd\sin\theta$. If the phase, Ψ, is zero, then all the elements add, and we get a strong signal. As Ψ increases, the vectors are out of phase, and the sum will decrease. For the case $N\Psi=2\pi$, the sum is zero. This corresponds to: $Nkd\sin\theta = 2\pi$, or more generally

$$Nkd\sin\theta = 2m\pi, \qquad \text{where m= 1,2,3, ...} \qquad \text{(Eqn. 8.8)}$$

This defines the zeroes in the beam pattern. For a continuous antenna element, the sum is replace by an integral over an antenna of length L:

$$E(\theta) \approx \int_{-\frac{L}{2}}^{\frac{L}{2}} a(x)e^{-ik\sin\theta}\,dx = \int_{-\frac{L}{2}}^{\frac{L}{2}} e^{-ik\sin\theta}\,dx = L\frac{\sin(kL\sin\theta/2)}{kL\sin\theta/2} \qquad \text{(Eqn. 8.9)}$$

The power at any particular location will then be proportional to the square of the electric field strength.

Figure 8-9 shows this characteristic $\sin^2\alpha/\alpha^2$ shape, with zeros where the argument of sin is mπ, or :

$$kD\sin\theta/2 = m\pi$$
$$\Rightarrow kD\sin\theta = 2m\pi \qquad \text{(Eqn. 8.10)}$$

This leads to:

$$\frac{2\pi}{\lambda} D\sin\theta = 2m\pi \quad \Rightarrow D\sin\theta = \lambda, \text{ or}$$

$$\frac{\lambda}{D} = \sin\theta \qquad \text{(Eqn. 8.12)}$$

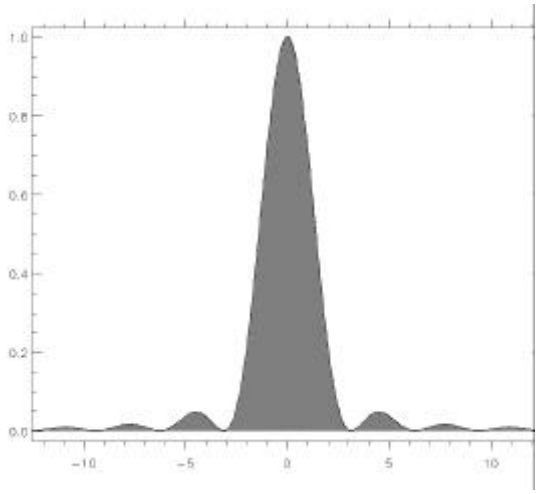

Figure 8-9. The square of the sinc function: $\sin^2(\alpha)/\alpha^2$

This is effectively the same result as we inferred for the resolution of diffraction limited optics- and the reasons are the same!

The equation for determining azimuth resolution (R_a) is

$$R_a = \frac{\lambda R_s}{D_a} \qquad \text{(Eqn. 8.13)}$$

where: λ= operating wavelength,
R_s = slant range to the target, and
D_a= length of the antenna.

The relationships expressed in Equation 8-13 show that:
(1) azimuth resolution decreases in proportion to increasing range (i.e., resolution is best in near range, where the width of the beam is narrowest), and
(2) a long antenna or a short operating wavelength will improve azimuth resolution.

The latter two parameters both enable the radar beam to be focused into a narrower angle; beam spreading is inversely proportional to antenna length and directly proportional to wavelength. There are several ways to obtain improved azimuth resolution with conventional RARs: a long antenna, a short operating wavelength, or a close-in range interval. However, the practical limit of antenna length for aircraft stability is about 5 m, and the all-weather capability of radar is effectively reduced when the wavelength is decreased below about 3 cm. Because of these limitations, RARs are best suited for low-level, short-range operations.

The resolution of a real aperture, imaging radar is, in the along track direction, given above can be rewritten as:

$$R_a = \frac{\lambda h}{L \cos\theta} \qquad \text{(Eqn. 8.14)}$$

For ordinary space kinds of numbers (antenna length L = 10 m, λ=3 cm, h = 800 km, θ=20°) we get a resolution of 2.5 km. We need a bigger antenna!

Before proceeding to the method by which a long synthetic antenna can be constructed, we look briefly at some real antenna patterns, again from the SIR-C X-SAR instrument. Figure 8-10 shows what certainly appears to be a sinc^2 pattern, per the theory described above (note that the use of dB as a unit means that we have a logarithmic vertical axis). A companion figure, Figure 8-11, shows the data on a linear vertical scale (bottom), and divided by the expected factor of $\text{sinc}^2\left(\frac{f}{0.151^o}\right)$ in the top. Here, the model is for the 3-cm (9.6 GHz) waves, given the 12-meter antenna length ($0.151° = \frac{l}{L}$).

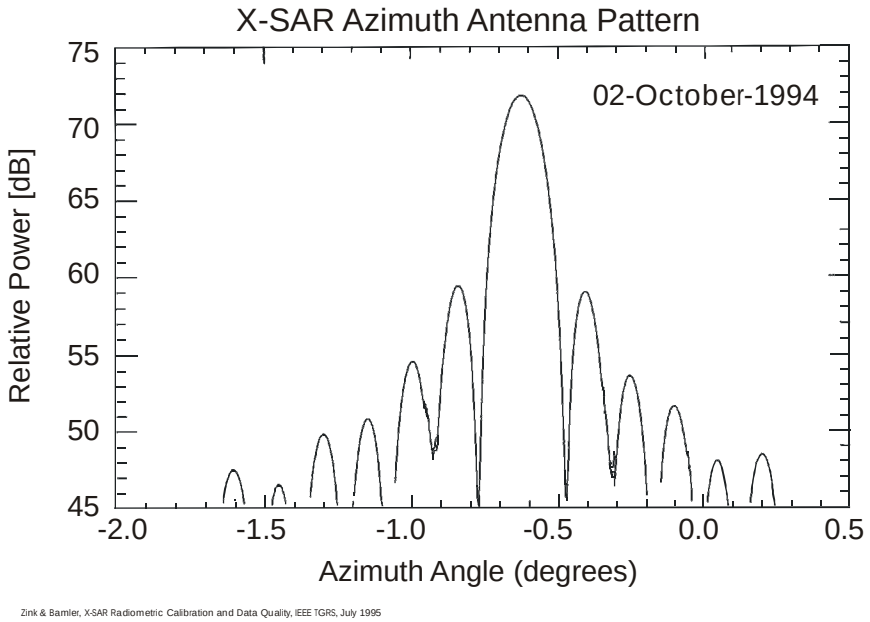

Figure 8-10. SIR-C X-SAR azimuthal antenna pattern as observed from ground observations along the beam centerline (the center of the range antenna pattern).

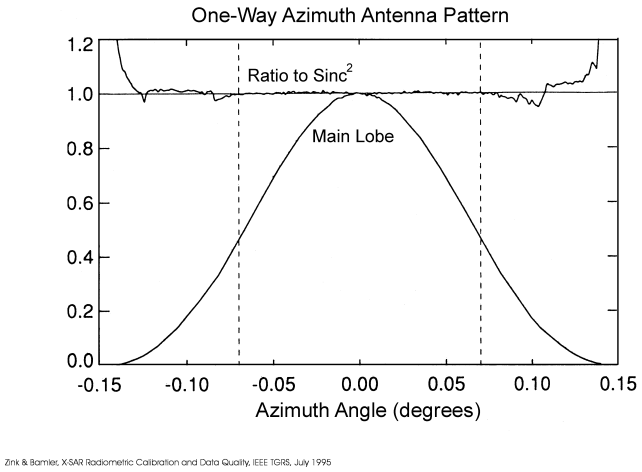

Figure 8-11. SIR-C X-SAR azimuthal antenna pattern on a linear scale, and compared to Sinc2. Note that the portion of the data processed come from the region between the dashed lines $\left(\pm 0.07^{o}\right)$, for which the model is very accurate.

For comparison, the range (or elevation) antenna pattern, synthesized from a number of observations like those shown in Figure 8-10, is given in Figure 8-12. Note that the width is considerably greater, given the relatively narrow dimension of the antenna in the corresponding direction (0.75 m)

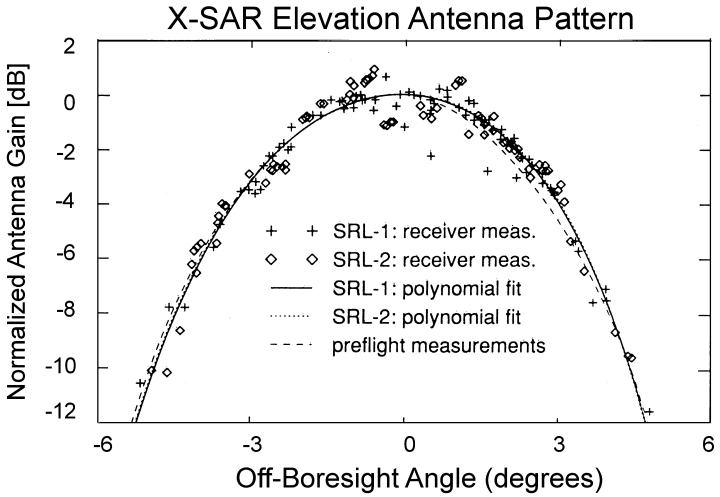

Figure 8-12. SIR-C X-SAR range antenna pattern. This beam pattern needs to cover the entire cross-track range of the system - here 20-70 km as illuminated from 222 km altitude.

C Synthetic Aperture Radar

The principal disadvantage of real-aperture radar is that its along-track or azimuth resolution is limited by antenna length. Synthetic-aperture radar (SAR) was developed to overcome this disadvantage. SAR produces a very long antenna synthetically or artificially by using the forward motion of the platform to carry a relatively short real antenna to successive positions along the flight line. The longer antenna is simulated by using the coherence of radar signals. If the sensor is moving at velocity v, and has an antenna length L, then the main beam footprint on the surface has a characteristic length $\ell = \frac{2\lambda h}{L}$. Data are accumulated for as long as a given point on the ground is in view (see figure 8-13)

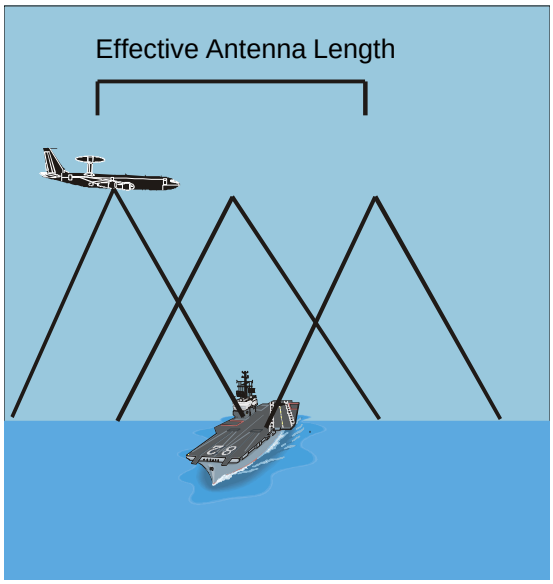

Figure 8-13

Magically, the synthesized collection of measurements will have a beam width equal to

$$\theta_s = \frac{\lambda}{\ell} = \frac{L}{2h} \qquad \text{(Eqn. 8.15)}$$

and the resulting array footprint on the ground has the size:

$$R_a = h\theta_s = \frac{L}{2} \qquad \text{(Eqn. 8.16)}$$

This very counter-intuitive result is due to the fact that for a smaller antenna (small L), the target is in the beam for a longer time. The time period that an object is illuminated increases with increasing range, so azimuthal resolution is range independent

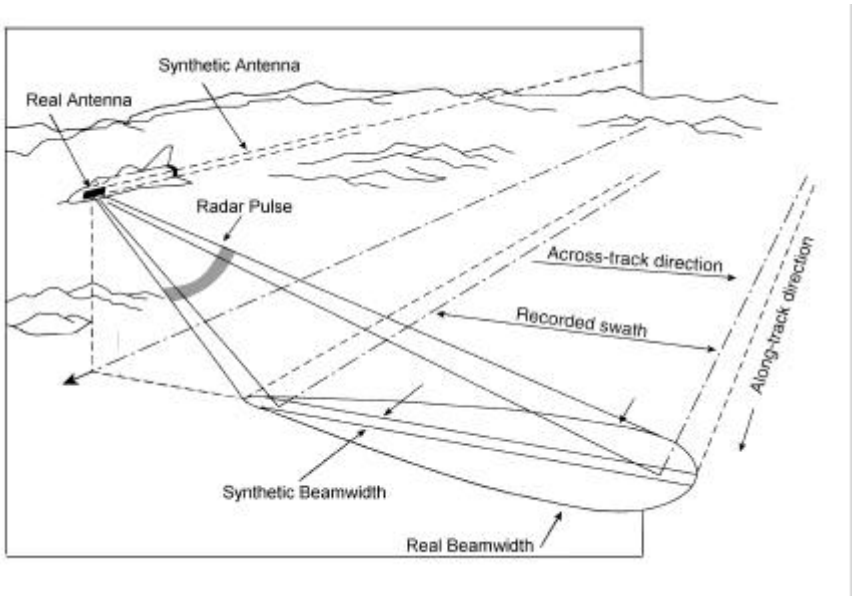

Figure 8-14 The synthetic antenna's length is directly proportional to range – as across-track distance increases, antenna length increases. This produces a synthetic beam with a constant width, regardless of range

The azimuth details are determined by establishing the position-dependent frequency changes or shifts in the echoes that are caused by the relative motion between terrain objects and the platform. To do this, a SAR system must unravel the complex echo history for a ground feature from each of a multitude of antenna positions. For example, if we isolate a single ground feature, the following frequency modulations occur as a consequence of the forward motion of the platform:

(1) The feature enters the beam ahead of the platform and its echoes are shifted to higher frequencies **(positive Doppler);**
(2) when the platform is perpendicular to the features position, there is no shift in frequency **(zero Doppler);** and
(3) as the platform moves away from the feature, the echoes have lower frequencies **(negative Doppler)** than the transmitted signal.

The Doppler shift information is then obtained by electronically comparing the reflected signals from a given feature with a reference signal that incorporates the same frequency of the transmitted pulse. The output is known as a **phase history,** and it contains a record of the Doppler frequency changes plus the amplitude of the returns from each ground feature as it passed through the beam of the moving antenna.

D Radar Cross Section (s)

The radar cross section, σ, is generally defined as the ratio of the backscattered energy to the energy that the sensor would have received if the target surface has scattered the energy incident on it in an isotropic fashion. The backscatter cross section is usually expressed in dB (decibels), which is given by: σ = 10 log (energy ratio) (Elachi, page 163). A rough idea of the magnitude of σ is given by Figure 8.15 (Elachi, page 175), which shows the scattering coefficients inferred from Skylab data at 13.9 GHz, at 33° incidence - something like 30% of the energy is returned (-10 dB±3dB), it would seem, though there are some subtleties to the reference point to be used.

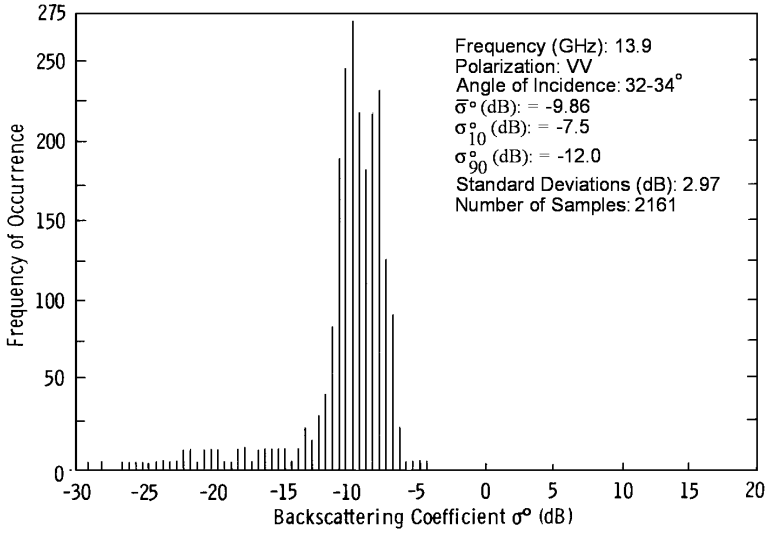

Figure 8-15

σ depends on any number of surface characteristics, with a strong dependence on the incident angle, and scattering angle. At scattering angles larger than about 30°, the surface scattering is dominated by the effect of small scale roughness (here, small scale means small compared to the wavelength). The "point scatterer" model is invoked here, and the small scatterers are assumed to make up a Lambertian distribution (an optics term)

$$\sigma(\theta) \propto \cos^2\theta \qquad \text{(Eqn. 8.17)}$$

This gives some idea of the type of functional dependence on angle one might obtain. The details are much messier. Observationally, the dependence is well illustrated by the Skylab results shown in Figure 8.16 (Elachi, page 176). The center line is the average, the two boundary lines show the 10 and 90 percentile bounds. Note the 10-15 dB variation in return with angle.

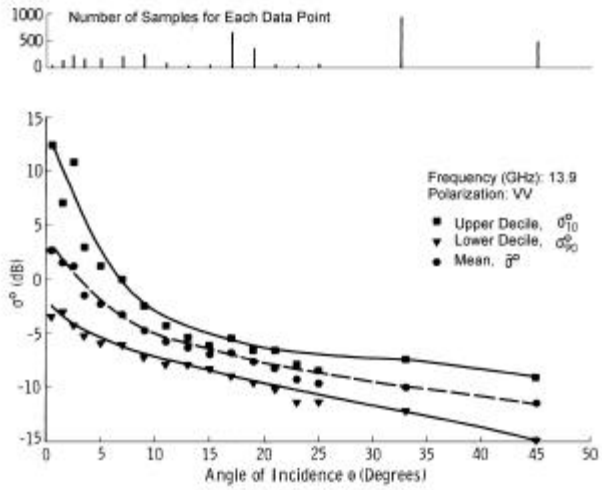

Figure 8-16

The point of this portion of the discussion is that the radar return has a strong dependence on the angle of incidence on the target surface. This differs fairly substantially from the optical case, where there are modest effects due to the illumination angle, aside from shadows. Note also that a sun-synchronous satellite (e.g. LANDSAT) always observes under roughly the same illumination conditions, whereas a radar satellite will not (theta varies).

Not included here is the form of the strong return which is observed if the wavelength of the incident radiation matches the characteristic scale length of features in the target. Strong returns are seen under this condition, termed Bragg scattering.

1 Dielectric Coefficient - soil moisture

The amplitude of the radar return depends strongly on the dielectric coefficient of the surface material (think index of refraction in normal optics, $n \sim \sqrt{e_r}$, the index of refraction varies as the square root of the relative dielectric constant). Radar returns vary substantially as the surface materials go from insulator to conductor - which in the dielectric coefficient shows up as the imaginary component, e''. In the illustration here, we see that soil moisture drives the imaginary term up, causing increased absorption of the radar energy. Note the wavelength dependence of this variation - higher frequencies (lower wavelengths) are affected more. This means lower frequencies are better for penetration of the ground and foliage.

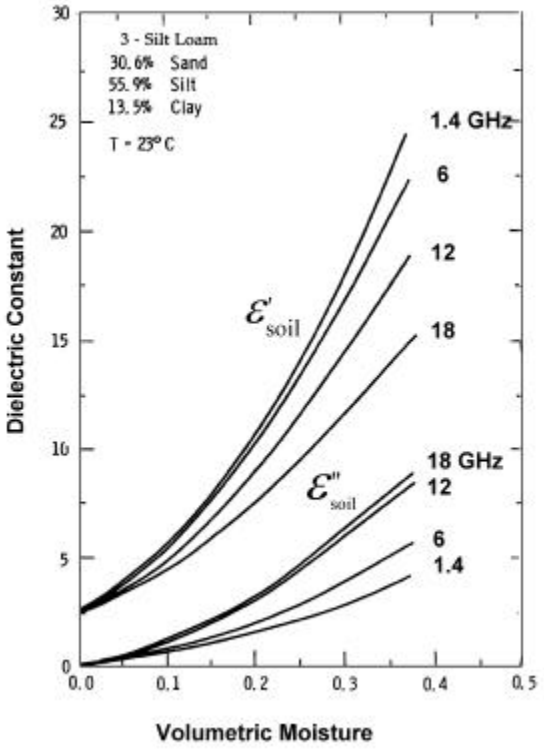

Figure 8-17. (left) The real $\Re e'\Im$ and imaginary $\Re e''\Im$ components of the dielectric coefficient for a silty loam mixture, as a function of water content. Both refraction and absorption increase with moisture content.

Figure 8-18 (below) The concept of rough and smooth needs to take into account the wavelength of the radiation

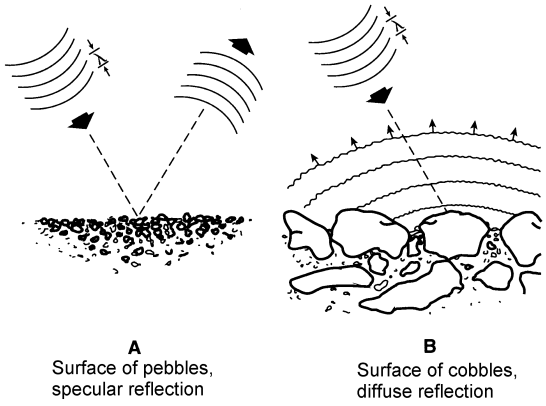

2 Roughness

The effect of surface roughness is illustrated by Figure 8-18. (Elachi, page 174, Sabins pages 197-201). The figure is somewhat schematic, but it emphasizes the variation in radar return with angle, and surface roughness. Note that this roughness is relative to the wavelength, so smooth means surfaces like concrete walls, (e.g. cultural objects), rough tends to mean things like vegetation.

3 Tetrahedrons / Corner Reflectors

Hard targets, meaning most man-made artifacts, generally have sharp corners and flat surfaces. These produce extremely bright returns, often saturating the images produced from SAR systems. The SIR-C flight over Death Valley included calibration sequences with retro-reflectors, which have as a characteristic that they return all incident radiation back in the direction of incidence - that is, they are nearly perfect reflectors. Figure 8-19 shows some SIR-C observations rendered in line graphics. In the SAR images, these correspond to a small white dot against the relatively flat background.

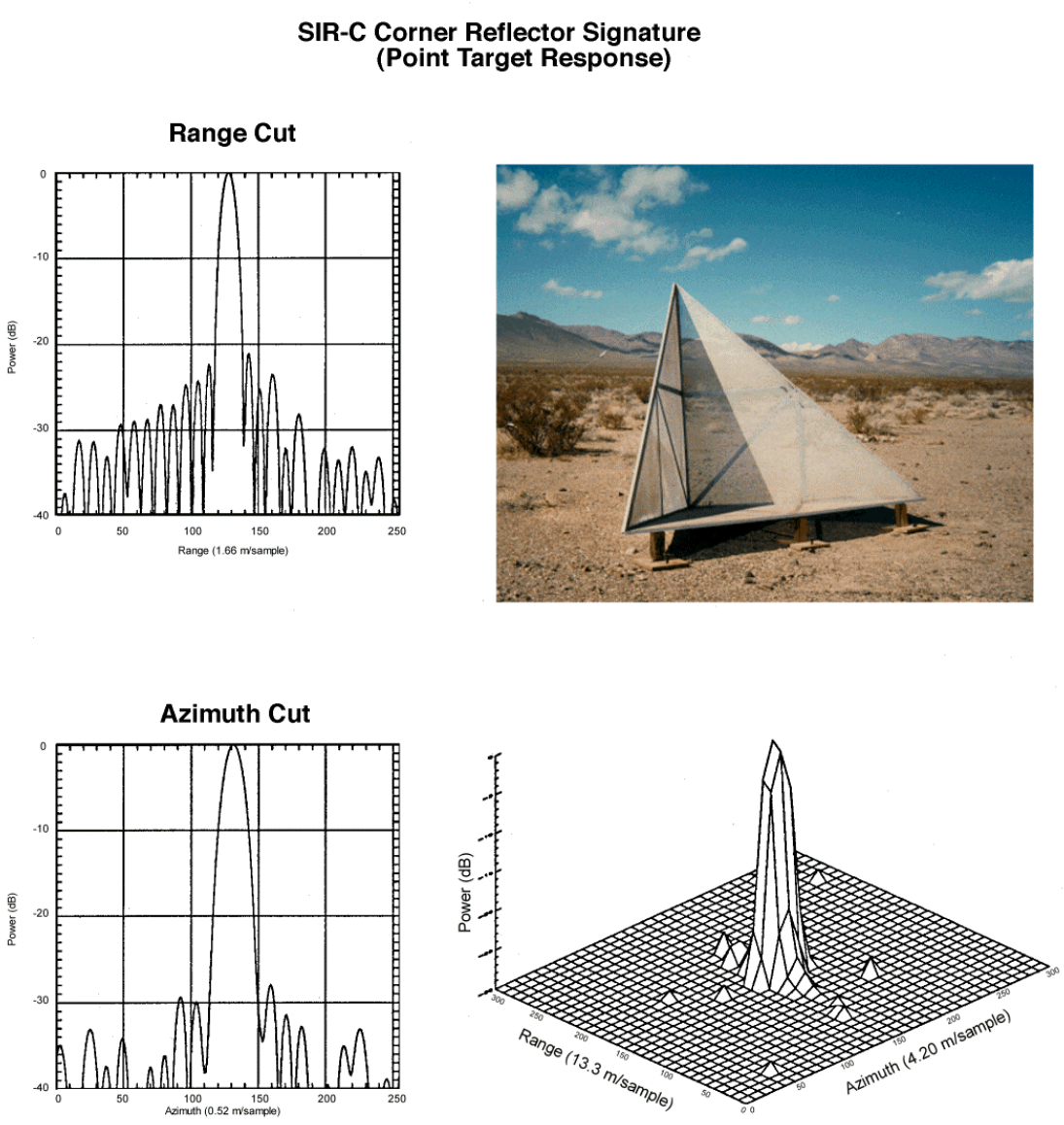

Figure 8-19. SAR impulse response

E Polarization

The above discussion ignores the important topic of polarization. Radar transmissions are polarized, with components normally termed vertical (V) and horizontal (H). Vertical means that electric vector is in the plane of incident, horizontal corresponds to the state where the electric vector is perpendicular to the plane of incidence. (Elachi, page 25). The receive antenna, in turn, can be selected for either V or H returns. This leads to a possible matrix of return values:

$$s = \begin{pmatrix} S_{HH} & S_{HV} \\ S_{VH} & S_{VV} \end{pmatrix}$$

Where the first subscript is determined by the transmit state, the second by the receive state. These four complex (amplitude **and** phase) components of the scattering matrix give a wealth of information, much more than can be obtained from an optical system. Generally speaking, scatterers which are aligned along the direction of polarization give higher returns, rough surfaces produce the cross-terms. Water gives almost zero scattering in the cross terms. Several illustrations have been given above which show the difference in returns associate with the different polarizations.

F Wavelength

Notes on microwave wavelengths in RADARSAT/PCI notes, page 11, 43.

1) Radar penetrates clouds, smoke rain, haze. There is some wavelength dependence for rain penetration - at 15 cm and longer (2GHz and below), rain is not a problem. At 5 GHz (6 cm), significant rain shadows are seen. At 36 GHz (0.8 cm) moderate rainfall rates can cause significant attenuation.

2) Response to macroscopic structure, bulk electrical properties: X, C band primarily interacts with surface, L&P penetrate canopy, soil.

Band Designation*	Wavelength (cm)	Frequency (GHz)
Ka (0.86 cm)	0.8 - 1.1	40.0 - 26.5
K	1.1 - 1.7	26.5 - 18.0
Ku	1.7 - 2.4	18.0 - 12.5
X (3.0, 3.2 cm)	2.4 - 3.8	12.5 - 8.0
C	3.8 - 7.5	8.0 - 4.0
S	7.5 - 15.0	4.0 - 2.0
L (23.5, 25 cm)	15.0 - 30.0	2.0 - 1.0
P	30.0 - 100.0	1.0 - 0.3

* Wavelengths commonly used in imaging radars are indicated in parenthesis.

G Vehicles

1 Shuttle Imaging Radar (SIR)

The shuttle imaging radar has flown in several versions (A, B, C), and twice as SIR-C on Endeavour - the first as SRL-1: STS-59, April 9 - 20, 1994, the second as SRL-2: STS-68, September 30 - October 11, 1994. Both missions were conducted with highly inclined orbits (57° inclination) in order to maximize the earth regions covered. The orbit was 222-km altitude, circular. The mission included X, C, and L band radar, and was capable of various modes including full polarimeteric (VV, VH, HV, and HH polarization).

Spatial resolution varied between the sensors, and with operating mode, but was generally from 10-25 meters, with a spatial extent of 30-50 km. The combined SIR-C/X-SAR payload had a mass (instruments, antennas, and electronics) of 10,500 kg filling nearly the entire cargo bay of the Shuttle.

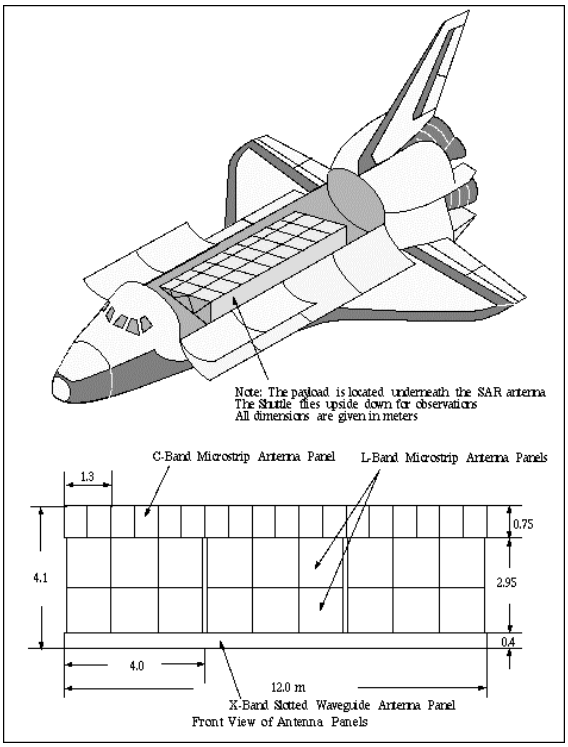

Figure 8-20.

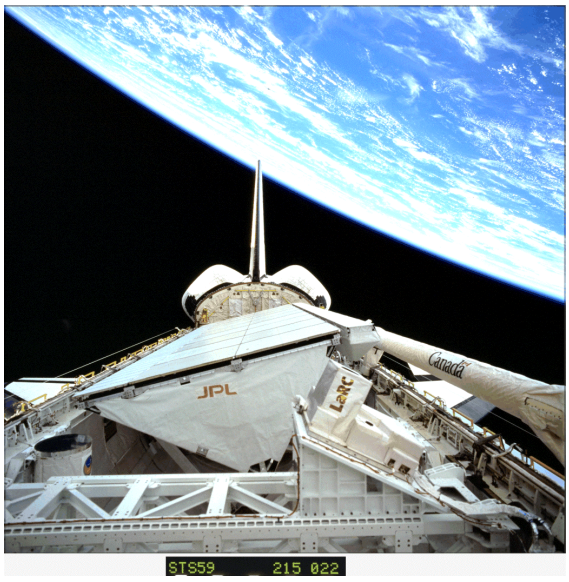

Figure 8-21.

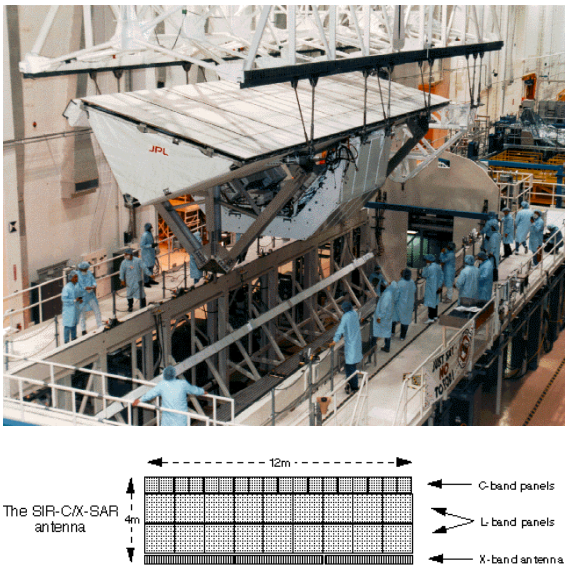

Figure 8-22.

Enormous data rates are implicit in these missions. Launched April 9, 1994, the STS-59 mission for SIR-C/X-SAR collected a total of 65 hours of data during the 10 day mission, roughly corresponding to 66 million square kilometers (26 million square miles). All data were stored onboard the shuttle using high-density, digital, rotary-head tape recorders. The data filled 166 digital tape cartridges (similar to VCR tape cassettes).

The mission returned 47 terabits of data (47×10^{12} bits). When all the radars are operating they produce 225 million bits of data per second, or the equivalent of 45 simultaneously operating television stations. The raw data was processed into images using JPL's digital SAR processor and by processors developed by Germany and Italy for the X-SAR data.

The L-Band and C-Band SARs allow multifrequency and multipolarization measurements. Parallel image generation in L-Band and C-Band with HH, VV, HV, or VH polarization. Look angle = variable from 20 - 55°. Data rate = 90 Mbit/s for L-Band and 90 Mbit/s for C-Band (a total of 4 streams of V and H data, each data stream has a data rate of 45 Mbit/s).

X-SAR (SAR for X-Band measurement provided by DARA/DLR and ASI) X-SAR uses only vertical polarization (VV). Look angle (off nadir) = 15 - 55°. Data rate = 45 Mbit/s. The X-SAR antenna transmits and receives vertically polarized signals; it can be tilted to achieve a range of look angles from 15° - 55°. The ground area illuminated by the antenna is an ellipse of about 60 km x 0.8 km (altitude of 222 km). The X-SAR electronics are mounted underneath the antenna on a cold plate structure. A TWT (Travelling Wave Tube) amplifier is transmitting up to 1736 pulses/s at peak transmit power of 3.35 kW. The pulses are frequency modulated (chirp) with a pulse length of 40 μs and a programmable bandwidth of 9.5 or 19 MHz. The signal echoes are amplified in a coherent receiver, digitized (4 or 6 bit) and recorded together with auxiliary data.

Parameter	**L-Band**	**C-Band**	**X-Band**
Wavelength (cm)	23.5	5.8	3.1
Frequency	1.250 GHz	5.3 GHz	9.6 GHz
Aperture length Aperture width	12.0 m 2.95 m	12.0 m 0.75 m	12.0 m 0.4 m
Architecture	Active Phased Array		Slotted waveguide
Polarization	H and V	H and V	V
Polarization isolation	25 dB	25 dB	39 dB
Antenna gain	36.4 dB	42.7 dB	44.5 dB
Mechanical steering range	N/A	N/A	±23°
Electronic steering range	±20°	±20°	N/A
Elevation beamwidth	5-16°	5-16°	5.5°
Azimuth beamwidth	1.0°	0.25°	0.14°
Peak radiated power	4400 W	1200 W	3350 W
System noise temperature	450 K	550 K	551 K
Mass of structure	3300 kg		49 kg

2 RADARSAT

Radarsat data were briefly illustrated in Chapter 1, in figure 1-19. Radarsat carries a C-band synthetic aperture radar, and operates in HH polarization only. Launched on November 4, 1995, it has a five-year design life. There are 7 beam modes offering a wide range of resolutions (8 - 100 meters) and swath widths (50 - 500 km). Incidence angles vary from 20-59°. http://www.rsi.ca/classroom/cl_rsat.htm

The satellite is in a circular, sun-synchronous orbit (dawn-dusk), at 798-km altitude, 98.6° inclination, and with a 100.7-minute period. The circular orbit is maintained as accurately as possible to maintain repeatability in the imaging. This allows for the application of techniques in change detection, and interferometry.

The radar has a power transmission / duty cycle of 5 kW (peak); 300s W (average)/ up to 28%. The antenna is a 15 m x 1.5 m phased array. The pulse is 1270Hz - 1390Hz; PRF = 42 μs.

RADARSAT is a right-looking sensor, facing east during the ascending orbit and west during the descending orbit. The look direction can have a significant influence on the appearance of radar imagery especially when features have an organized linear structure (e.g., agricultural surfaces or geological structures).

3 European Radar Satellites, ERS-1, -2

The European Radar Satellites, ERS-1 and ERS-2, are also polar orbiting SAR systems. ERS-1 was placed in a near-polar orbit at a mean altitude of about 780-km, inclination of 98.52°, period of about 100 minutes. The instrument payload included active and passive microwave sensors and a thermal infrared radiometer. The satellite (see the figure) is large, weighing 2400 kg and measuring 12 m x 12 m x 2.5 m. ERS-1 ceased operation on 10 March 2000

Like Radarsat, the radar is C-band (5.3 GHz), but it operates in VV polarization. Incidence angle is 20-26°. It is somewhat more powerful than Radarsat, also; the peak power supplied to the payload is 2600 W, payload average power is at most 550 W - but the payload requires almost double that power when active. ERS-1 was launched on 17 July 1991 by an Ariane 4 from Kourou, French Guiana. The satellite masses are quite large: 2157.4 kg for ERS-1, 2516 kg for ERS-2. Over 320 kg of the mass goes to the SAR system.

Figure 8-23
ESA's ERS-1 satellite was photographed by the Spot-4 Earth observation satellite of the French space agency, CNES, at 09:56 UT on 6 May 1998. From its 820 km orbit, Spot-4 recorded ERS-1 passing by 41 km below at a relative speed of 250 km/h, over the Tenere Desert of Niger, Africa. Resolution of the ERS-1 spacecraft is 0.5 meters. The image was taken by one of the HRVIR (high-resolution visible-infrared) cameras during Spot's testing phase.

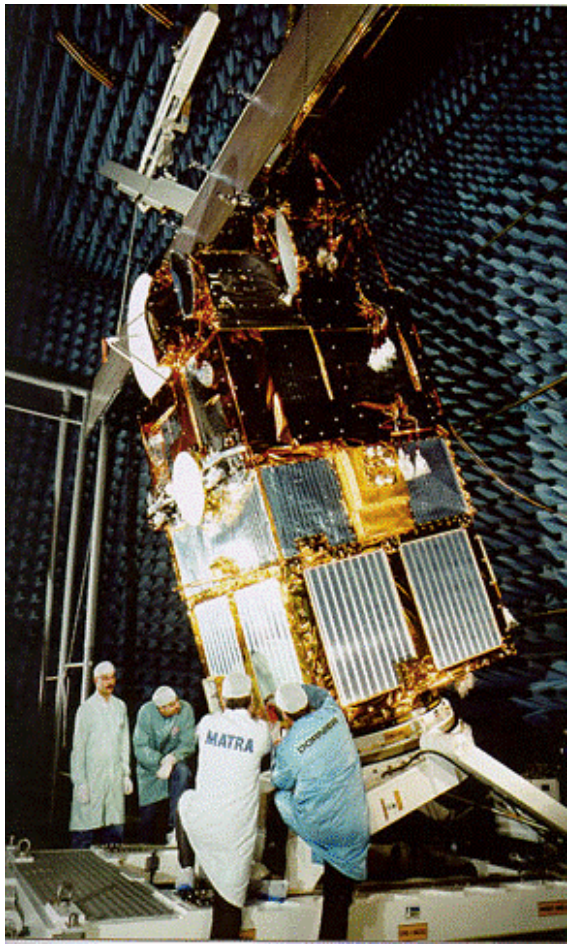

Figure 8-24 ERS-2

The satellite is 11.8 m in total height. The solar array consists of two 5.8 m x 2.4 m wings, manufactured from flexible reinforced Kapton, on which are mounted a total of 22,260 solar cells. The two solar array wings are deployed by means of a pantograph mechanism, and the whole array rotates through 360 degrees with respect to the satellite during each orbit in order to maintain its Sun pointing.

ERS-1 was launched on 17 July 1991 into a sun-synchronous, near polar, near circular orbit at a mean altitude of 785 km and an inclination of 98.5 degrees. The vehicle was 3-axis stabilized, with orbit knowledge: 5 m (radial), 15 m (cross) 60 m (along). Substantial data-rates are again implicit. The data down link is x-band (105 Mbit/s high rate link for AMI image mode) X-band (15 Mbit/s low rate link for real-time and playback of LBR data) on-board recorders provide 6.5 Gbits storage S-band telemetry links for housekeeping data.

ERS-2 was built by a consortium led by Deutsche Aerospace and was launched on April 20, 1995 on an Ariane. The ERS-2 satellite is essentially the same as ERS-1 except that it includes a number of enhancements and it is carrying a new instrument to measure the chemical composition of the atmosphere, named the Global Ozone Monitoring Experiment (GOME).

a Multi-temporal images - Rome

This multi-temporal image of Rome and the Castelli Romani hills to its southeast shows, by its colors, a variety of changes, both in the agricultural fields of the lowlands, and in the grasslands and forests of the hillier areas. The city, however, has not changed in the short interval between the capture of the first and the last of the images and thus appears more uniformly gray, as equal values of the RGB colors from which the image is made give a range of grayscales rather than of colors.

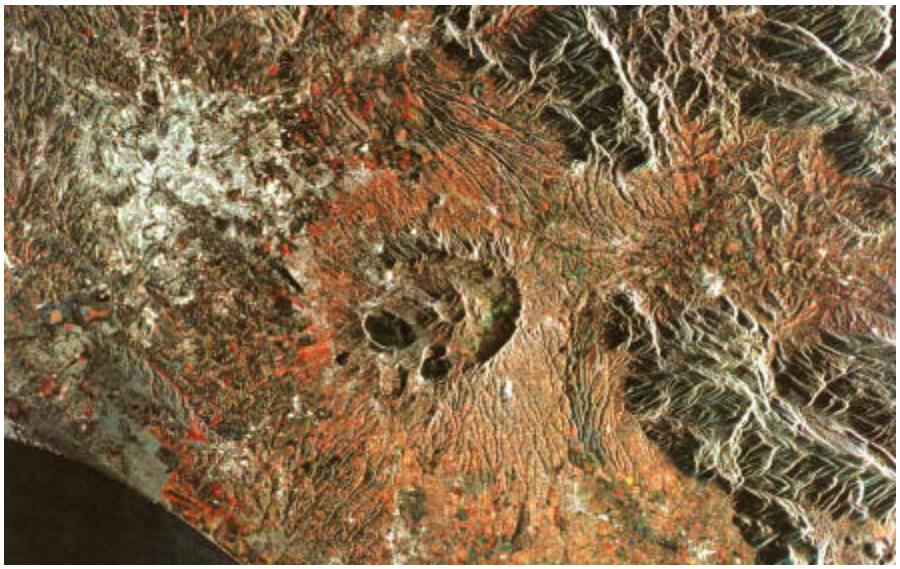

Figure 8-25. Incidence Angle: 23 degrees; Spatial Resolution: 30 meters; Swath Width: 100 kilometers. Copyright © ESA, 1995 Original data distributed by Eurimage
http://www.eurimage.it/Products/ERS/Msample_images.shtml

b SPAIN - MOROCCO - Strait of Gibraltar

This spectacular image of the Strait of Gibraltar shows internal waves (wavelength about 2 km) which seem to move from the Atlantic Ocean to the Mediterranean Sea, at the east of Gibraltar and Ceuta. Internal waves are usually created by the presence of two different layers of water combined with a certain configuration of relief and current. In the case of the Strait of Gibraltar, the two layers correspond to different salinities, whereas the current is caused by the tide passing through the Strait. As this current meets the ascending ocean bottom in the Strait, the internal waves are generated reaching the surface some kilometers behind the Strait. They are not directly visible to the observer but produce a perturbation at the surface that appears as strips of rough and calm water. ERS-1 therefore gives scientists the opportunity to observe and map such phenomena.

The image has been artificially colored - land encoded as shades of brown, water as shades of blue; the data were acquired at the Fucino ground station on 7-1-1992;

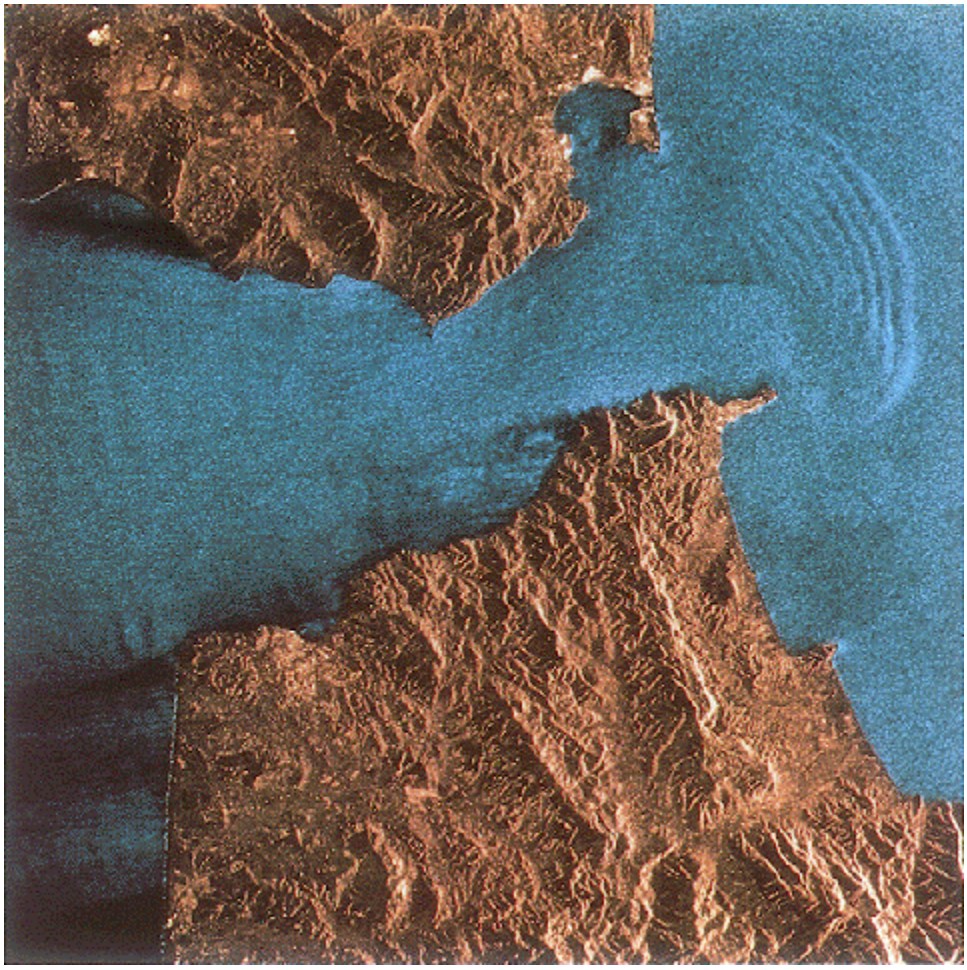

Figure 8-26. Straits of Gibraltar, Area covered 90 km x 100 km; C-VV; Resolution: 30 m.

H Problems

1. For a SAR system, such as SIR-C, does the nominal 12.5 meter azimuthal resolution for the German X-band system correspond well to the nominal antenna width? What pulse length would be required to match that in range resolution?

2. What wavelengths and polarizations are used for the commercial SAR systems (Radarsat, ERS)?

3. For a spotlight mode SAR system, what azimuthal resolution could be obtained with x-band for a 10 second integration interval (assume v = 7 km/s)

4. For the conditions illustrated in Figure 8-12, the shuttle was at 222 km altitude, and the antenna (shuttle) attitude was 27.1°. What range does the $27.1^o \pm 3^o$ (measured from nadir) correspond to?

5. During an earlier shuttle flight (SIR-B), observations similar to those shown in Figures 8-10 to 8-12 were made. Given a vehicle velocity of 7.5 km/s, convert the variations in time displayed here into a beam width in degrees. The wavelength is 23.5 cm. The local angle of incidence is 31°. (The incidence angle is measured down from the vertical.) What is the antenna length implied by this antenna pattern?

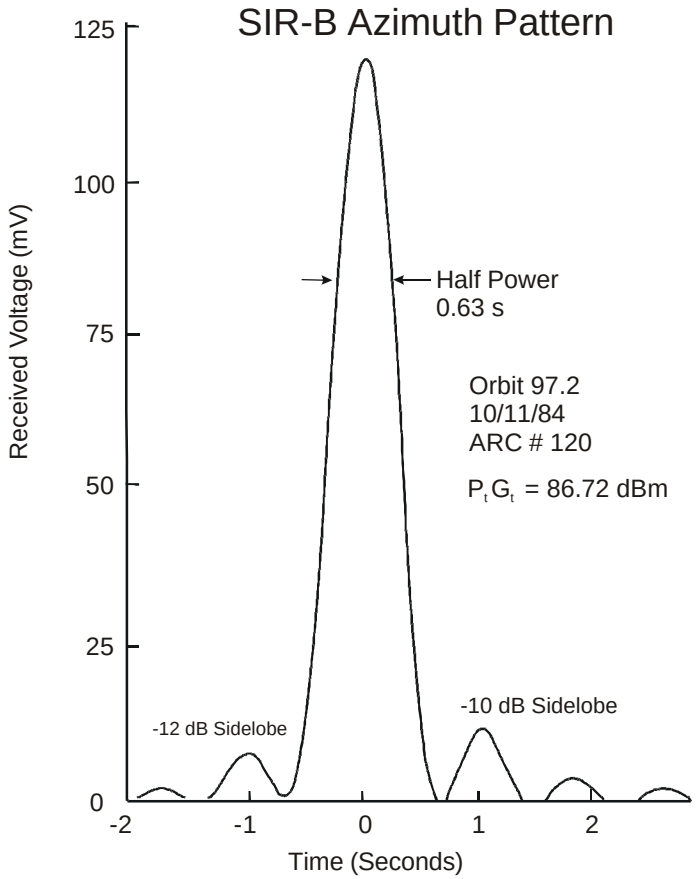

Dobson et al: External Calibration of SIR-B Imagery, IEEE TGRS, July 1986

Figure 8-27. SIR-B azimuth (along track) antenna pattern.

6. The decrease in radar energy as the beam propagates is illustrated by an example from the SIR-B mission, which shows the results of measuring the variation in power observed at depths of 12 and 35 cm in desert soil (near Mina, NV), from a paper by Farr et al. 1986. If the radar energy has decreased by 8 dB in the first 12 cm, what is the characteristic scale length, d, as defined here? This scale length is determined by the imaginary part of the dielectric coefficient.

$$I = I_o \, e^{-x/d}$$